PHYSICAL REVIEW C, VOLUME 65, 041304(R)

Surface effects in nuclear Cooper pair formation

N. Giovanardi,[1,2,†] F. Barranco,[3] R. A. Broglia,[1,2,4] and E. Vigezzi[2]
[1]*Dipartimento di Fisica, Università di Milano, via Celoria 16, I-20133 Milano, Italy*
[2]*Istituto Nazionale di Fisica Nucleare, via Celoria 16, I-20133 Milano, Italy*
[3]*Departamento de Fisica Aplicada, Escuela Superior de Ingenieros, Universidad de Sevilla, Spain*
[4]*The Niels Bohr Institute, University of Copenhagen, Blegdamsvej 17, DK-2100 Copenhagen, Denmark*
(Received 21 February 2001; published 25 March 2002)

The formation of Cooper pairs resulting from the exchange of vibrations between pairs of fermions moving in time reversal states close to the Fermi surface in a semi-infinite system of nuclear matter (slab model) with parameters adjusted so as to mimic real nuclei, leads to pairing gaps which account for a substantial fraction of the experimental value throughout the mass table. The predictions are in qualitative agreement with detailed calculations carried out for finite nuclei and testify to the central role the surface of nuclei plays in the phenomenon of nuclear superfluidity.

DOI: 10.1103/PhysRevC.65.041304 PACS number(s): 21.30.Fe, 21.60.−n, 21.65.+f

It is well established that nuclear superfluidity is mainly a surface effect, as demonstrated by the behavior of the $^1S_0$ phase shift of nucleons which is large (attractive) at low densities (relative kinetic energies) typical of the nuclear surface, becoming zero and eventually negative (repulsive) at saturation densities. It is equally well known that nucleons moving close to the Fermi energy display an effective ω-mass $[m_\omega=(1+\lambda)m]$, due to the coupling of nucleons to surface vibrations, which is considerably larger than the bare mass m. Typical values of the mass enhancement factor λ for both spherical [1] and deformed [2] nuclei lie in the range $0.4\leqslant\lambda\leqslant 0.8$ and arise essentially from the coupling of nucleons to low-lying collective surface vibrations of multipolarity $J\leqslant 5$. In keeping with the fact that the electron-phonon induced pairing gap in Bardeen-Cooper-Schrieffer (BCS) theory [3] is given by $\Delta=2\hbar\omega_D\exp(-1/\lambda)$ and of the fact that $\hbar\omega_D$ in nuclei is of the order of few MeV, one expects the induced interaction arising from the exchange of surface vibrations between nucleons moving in time reversal states lying close to the Fermi energy, to be responsible for a conspicuous part of the nuclear pairing gap. This expectation has been confirmed by detailed calculations [4].

To shed light on the universality of these results, we shall study the induced pairing interaction in a system free of shell effects, but retaining the properties associated with the confinement by an elastic surface. For this purpose, use will be made of the slab model [5,6], that is a semi-infinite system of nuclear matter. In it, nucleons are confined in the half-space $z<0$ by the one dimensional Fermi-like potential

$$V(z)=V_0(1+e^{-z/a})^{-1}. \tag{1}$$

Here $V_0=45$ MeV is the depth of the potential and $a=0.75$ fm is its diffusivity. The single-particle wave functions can be written as

$$\Phi_\nu(\boldsymbol{r})=e^{i\boldsymbol{k}_{\nu p}\cdot\boldsymbol{r}_p}\phi_\nu(z), \tag{2}$$

the corresponding energy eigenvalues and momentum parallel to the surface being $\epsilon_\nu=\hbar^2k_{\nu p}^2/2m+\epsilon_{\nu z}$ and $\boldsymbol{k}_{\nu p}=(k_{\nu x},k_{\nu y},0)$, respectively. The vector $\boldsymbol{r}_p$ lies also on the plane parallel to that of the surface of the slab $(x,y,0)$. The wave functions $\phi_\nu(z)$ are solutions of the single-particle Schrödinger equation

$$\left(\frac{-\hbar^2}{2m}\frac{d^2}{dz^2}+V(z)\right)\phi_\nu(z)=\epsilon_{\nu z}\phi_\nu(z), \tag{3}$$

normalized so that, for $z\rightarrow-\infty$,

$$\phi_\nu(z)=\sqrt{2}\cos(k_{\nu z}z+\theta_\nu), \tag{4}$$

where $k_{\nu z}$ is the asymptotic wave number and θ_ν a phase.

The next step in the calculation of the induced interaction consists in determining the vibrational modes of the system. For this purpose and following Refs. [4,5], we diagonalize, in a particle-hole basis and in the harmonic approximation (RPA) the surface-peaked separable interaction

$$v(\boldsymbol{r},\boldsymbol{r}')=k_0 g(|\boldsymbol{r}_p-\boldsymbol{r}'_p|)V'(z)V'(z'), \tag{5}$$

where $V'(z)$ is the derivative of the potential defined in Eq. (1). The finite range Yukawa interaction acting in the x,y direction,

$$g(|\boldsymbol{r}_p-\boldsymbol{r}'_p|)=\frac{e^{-|\boldsymbol{r}_p-\boldsymbol{r}'_p|/a_r}}{2\pi a_r|\boldsymbol{r}_p-\boldsymbol{r}'_p|}, \tag{6}$$

with $a_r=1$ fm, has been chosen so as to give a realistic value of the nuclear surface tension (1 MeV/fm^2) [5]. The coupling strength k_0 is determined by the relation [7]

$$k_0^{-1}=\int dz\rho'_0(z)V'(z), \tag{7}$$

which expresses the self-consistent condition existing between density and potential fluctuations associated with the

[†]Deceased.

normal modes. Diagonalizing the interaction given in Eq. (5) in the random-phase approximation (RPA) one can construct the linear response function

$$R^{RPA}(K,\hbar\omega)=\frac{R^0(K,\hbar\omega)}{1-k_0\tilde{g}(K)R^0(K,\hbar\omega)}. \tag{8}$$

It is written in terms of the unperturbed response $R^0(K,\hbar\omega)$ which, in the slab model, can be accurately parametrized by the functions

$$\mathrm{Re}R^0(\epsilon,K)=-N(K)\left(\frac{\epsilon-E_0(K)}{[\epsilon-E_0(K)]^2+\Gamma(K)^2}-\frac{\epsilon+E_0(K)}{[\epsilon+E_0(K)]^2+\Gamma(K)^2}\right), \tag{9}$$

and

$$\mathrm{Im}R^0(\epsilon,K)=\frac{N(K)}{\pi}\Gamma(K)\left(\frac{1}{[\epsilon-E_0(K)]^2+\Gamma(K)^2}-\frac{1}{[\epsilon+E_0(K)]^2+\Gamma(K)^2}\right), \tag{10}$$

in terms of the energy centroid $E_0(K)$, the width $\Gamma(K)$ and normalization strength $N(K)$ [cf. Eqs. (3.1)–(3.3) of Ref. [5]]. The function

$$\tilde{g}(K)=\frac{1}{\sqrt{1+(a_rK)^2}}, \tag{11}$$

is the kernel of the two-dimensional Fourier transform

$$g(|\boldsymbol{r}_p-\boldsymbol{r}'_p|)=\int\frac{d^2K}{(2\pi)^2}e^{i\boldsymbol{K}(\boldsymbol{r}_p-\boldsymbol{r}'_p)}\tilde{g}(K). \tag{12}$$

Let us now consider the process in which pairs of nucleons moving in time reversal states exchange the eigenmodes of Eq. (8). We shall denote $k_{\nu p}$ and $k_{\nu' p}$ the momentum of the single-particle states in the initial and in the final channels respectively, in a plane parallel to the surface. We shall denote with $k_{\nu z}$ and $k_{\nu' z}$ the asymptotic momentum along the z direction. The wave number $\boldsymbol{K}$ of the exchanged phonon is fixed by the relation expressing the parallel momentum conservation, that is

$$\boldsymbol{K}=\boldsymbol{k}_{\nu p}-\boldsymbol{k}_{\nu' p}. \tag{13}$$

The induced pairing matrix element can be written as [4]

$$v_{\nu\nu'}(K)=\frac{2}{\pi}[k_0\tilde{g}(K)]^2M_{\nu\nu'}^2\times\int_0^\infty d\hbar\omega\frac{\mathrm{Im}R^{RPA}(K,\hbar\omega)}{E_0-(|e_\nu|+|e_{\nu'}|+\hbar\omega)}. \tag{14}$$

Here $e_j\equiv\epsilon_j-\epsilon_F$, $(j=\nu,\nu')$, ϵ_F being the Fermi energy while

$$\epsilon_\nu\equiv\epsilon_{\nu p}+\epsilon_{\nu z}=\frac{\hbar^2k_{\nu p}^2}{2m}+\epsilon_{\nu z}, \tag{15}$$

$$\epsilon_{\nu'}\equiv\epsilon_{\nu' p}+\epsilon_{\nu' z}=\frac{\hbar^2}{2m}(\boldsymbol{k}_{\nu p}-\boldsymbol{K})^2+\epsilon_{\nu' z}, \tag{16}$$

and

$$M_{\nu\nu'}=\int dz\quad \phi^*_{k_{\nu' z}}(z)V'(z)\phi_{k_{\nu z}}(z). \tag{17}$$

To be noted that the finite range Yukawa interaction, acting in a plane parallel to the surface, suppresses the contributions to $v_{\nu\nu'}(K)$ associated with the short wavelength surface phonons (high K, corresponding to the high multipolarity surface vibrations in finite nuclei), as compared to a zero-range interaction [cf. Eqs. (11) and (14), setting $a_r=0$].

Within the framework of Bloch-Horowitz perturbation theory, the BCS number and gap equations [4]

$$N=2V\int\frac{d^3k}{(2\pi)^3}v^2(\boldsymbol{k}), \tag{18}$$

$$\Delta(\boldsymbol{k}_\nu)=\frac{2}{\pi}d^{-1}\int\frac{d^3k_{\nu'}}{(2\pi)^3}[k_0\tilde{g}(K)M_{\nu\nu'}]^2u(\boldsymbol{k}_{\nu'})v(\boldsymbol{k}_{\nu'})\times\int_0^\infty d\hbar\omega\frac{\mathrm{Im}R^{RPA}(K,\hbar\omega)}{E_0-(|e_\nu|+|e_{\nu'}|+\hbar\omega)}, \tag{19}$$

where

$$E_0=-\frac{V}{2}\int\frac{d^3k}{(2\pi)^3}u(\boldsymbol{k})v(\boldsymbol{k})\Delta(\boldsymbol{k}), \tag{20}$$

is the pairing energy, are self-consistently solved.

To be able to relate the corresponding results to the properties of finite nuclei of mass number A and radius $R=1.2A^{1/3}$ fm, the single-particle wave functions $\phi_\nu(z)$ have been normalized within a slice of thickness d [6]. Making use of the relation

$$V=S\cdot d, \tag{21}$$

where $V=\frac{4}{3}\pi R^3$ and $S=4\pi R^2$, one obtains

$$d=0.4A^{1/3}. \tag{22}$$

In Fig. 1(a) we show the state dependent pairing gap $\Delta(\boldsymbol{k}_\nu)$, solution of Eqs. (18)–(20), as a function of $\epsilon-\epsilon_F=(\hbar k_\nu)^2/2m-\epsilon_F$, averaged over all the single-particle states with the same value of k_ν^2 and for $R=6$ fm ($A\approx120$). It is seen that these results provide an overall account of the outcome of detailed microscopic calculations carried out for the nucleus ^{120}Sn (cf. Fig. 1, Ref. [4]), also shown in Fig. 1(a). As expected, the pairing gap is peaked at the Fermi surface, the associated FWHM reflecting the frequency distribution of the linear response of the system (cf. Fig. 2, Ref. [10]). In Fig. 1(b) we display the pairing gap associated with a particle at the Fermi energy as a function of

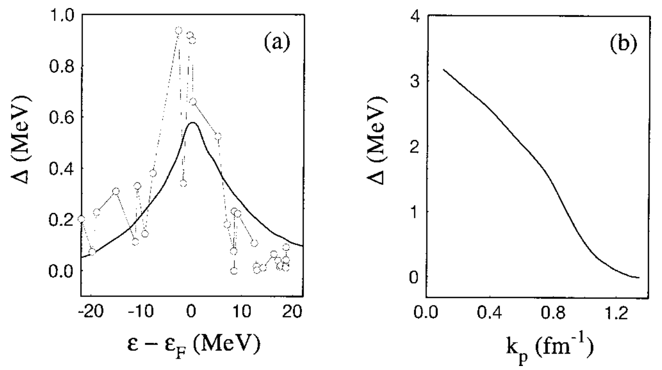

FIG. 1. (a) Pairing gap of particles as a function of the particle energy $\epsilon=(\hbar k_\nu)^2/(2m)$, for $R=6$ fm. For each energy value, the pairing gap Δ has been calculated as an average over the gaps of particles having the same k_ν^2. Detailed results for the nucleus ^{120}Sn are also displayed (open dots, cf. Fig. 1, Ref. [4]). (b) The pairing gap of a particle at the Fermi energy as a function of the momentum component parallel to the surface of the slab. The gap goes to zero when $k_{\nu p}=k_F=1.337$ fm^{-1}, corresponding to the case of particles moving parallel to the surface of the slab ($k_z=0$).

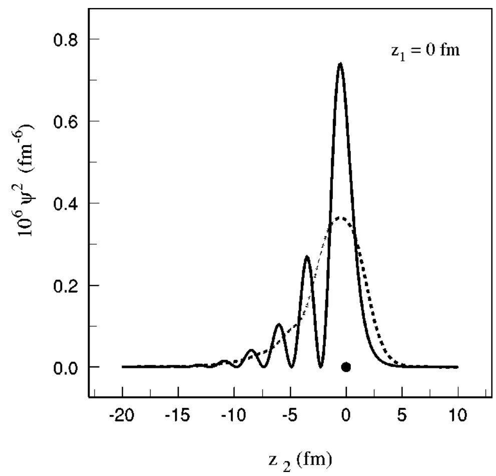

FIG. 3. Plot of ψ^2 [Eq. (25)], for $R=6$ fm and for particles with zero relative parallel coordinate ($R_p=0$), obtained fixing the coordinate of one particle (z_1, solid dot), as a function of the coordinate of the second particle (z_2). The surface of the slab is located at $z=0$. Also shown is the value of ψ^2 averaged over an interval of ≈ 5 fm (dashed curve).

the momentum component $k_{\nu p}$ lying in the (x,y) plane (parallel to the surface). The marked decrease of Δ as a function of $k_{\nu p}$ testifies to the surface origin of the induced pairing interaction $v_{\nu\nu'}$ [Eq. (14)].

While the relation given in Eq. (22) may be a reasonable way of determining the A dependence of $\Delta(\boldsymbol{k}_\nu)$, the precise numerical factor is uncertain. In fact, one can envisage a variety of prescriptions to work out a single number Δ out of results like those displayed in Fig. 1(a): (a) take the value of the lowest quasiparticle energy $[\Delta(\epsilon_F)]$, (b) average $\Delta(\boldsymbol{k}_\nu)$ over a given energy interval around the Fermi energy, etc. Following the prescription adopted in Ref. [4], we take an average of $\Delta(\boldsymbol{k}_\nu)$ over single-particle states with energy $|\epsilon_\nu - \epsilon_F| \leqslant 4$ MeV, an energy interval which is of the order of that spanned by the valence orbits in finite nuclei. As can be estimated from Fig. 1(a), this average reduces the pairing gap by about 20% from its peak value. Because of these differences, the comparison carried out below between Δ and the experimental data, can only be qualitative.

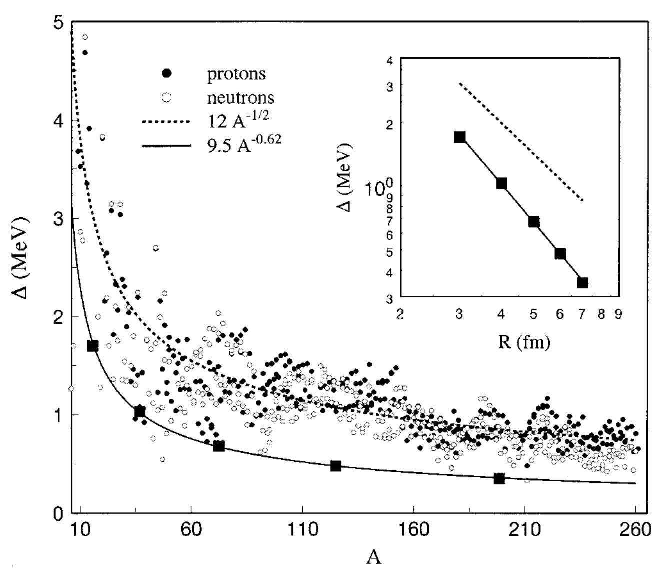

FIG. 2. The experimental pairing gap of neutrons (open dots) and protons (full dots) as a function of the mass number A, calculated from the nuclear binding energies reported in Ref. [9] through Eqs. (2-92) and (2-93) of Ref. [8], are well described, in average, by the function $\Delta_{exp}\approx 12A^{-1/2}$ MeV (dashed curve, Eq. (2-94) of Ref. [8]). The solid squares show the results of the self-consistent solution of Eqs. (18)–(20), results which are well fitted by the expression $\Delta=9.5A^{-0.62}$ MeV. In the inset, the same results are displayed as a function of the nuclear radius R in a log-log scale, to emphasize the different behavior of the two power laws.

The results of the average are well fitted by the power law (cf. inset in Fig. 2)

$$\Delta \approx \frac{9.5}{A^{0.62}} \text{ MeV}, \tag{23}$$

where the exponent of the mass number A is quite close to 2/3. This is a consequence of the $1/d$ dependence of Eq. (19), due to the surface character of the phonons exchanged by the nucleons, and of the nonlinear character of the pairing gap equation. Because the experimental values are reproduced, in average, by the parametrization (cf. Fig. 2)

$$\Delta_{exp} \approx \frac{12}{A^{0.5}} \text{ MeV}, \tag{24}$$

one concludes that $\Delta/\Delta_{exp}\approx 0.8/A^{0.12}$ MeV. In other words, the induced pairing interaction leads to pairing gaps which represent a substantial fraction of those experimentally observed, a result which is similar to that obtained in the case of detailed calculations in finite nuclei [4] [cf. also Fig. 1(a)].

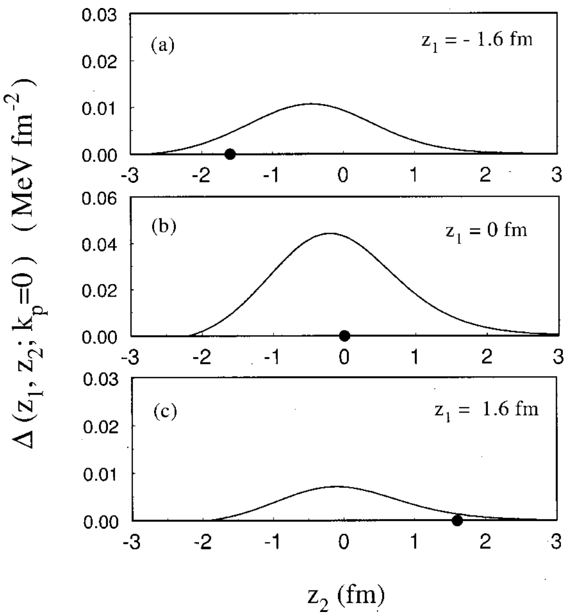

FIG. 4. Pairing gap calculated, for $R=6$ fm, as the product of the anomalous density ψ and the induced interaction v, as a function of the z coordinate of one of the two particles (z_2), giving the coordinate of the other particle (z_1) fixed values.

To account for the experimental pairing gap, one needs to add to the interaction $v_{\nu\nu'}$ [Eq. (14)] an extra contribution which we shall parametrize as G_0/A. We find that $G_0 \approx (0.5\pm 0.1)G$, where G/A is the strength of the pairing interaction which reproduces the experimental data [cf. Eq. (24) and Fig. 2, dotted curve]. In particular, in the case of $R=7$ fm, i.e., $A=200$, one obtains $G=27$ MeV, while $G_0=17$ MeV.

The results shown in Figs. 3 and 4 provide further insight into the role the surface of a confined Fermi liquid has in the formation of Cooper pairs. In Fig. 3, the modulus squared of the anomalous density (closely connected with the Cooper pair wave function)

$$\psi(z_1,z_2,R_p)=\int \frac{dk_p}{2\pi}k_pJ_0(k_pR_p)\int \frac{dk_z}{2\pi}\phi_{k_z}(z_1)\phi_{k_z}(z_2)\times u(k_p,k_z)v(k_p,k_z), \tag{25}$$

is shown as a function of the coordinate z_2 of one of the particles, fixing the coordinate $z_1(=0)$ of the other particle on the surface. In the above equation, J_0 is a Bessel function and R_p is the distance between particles in the direction parallel to the slab. The mean square radius $\langle r^2\rangle^{1/2} = (\int d^3r r^2|\psi|^2/\int d^3r|\psi^2|)^{1/2}$ of the Cooper pair is closely connected with the coherence length $\xi=\hbar v_F/\pi\Delta$ of the pair [11]. In keeping with the fact that $\epsilon_F\approx 36$ MeV, and that $\Delta\approx 0.6$ MeV at the Fermi energy [cf. Fig. 1(a)], one obtains, from this simple estimate, $\xi=28$ fm.

The pairing gap $\Delta(z_1,z_2,R_p)=v(z_1,z_2,R_p)\times\psi(z_1,z_2,R_p)$ is obtained multiplying the anomalous density by the induced interaction, defined in Eq. (14), a quantity which depends on e_ν and $e_{\nu'}$. For single-particle levels lying close to the Fermi energy we can neglect this dependence and write

$$v(z_1,z_2,R_p)=\frac{2}{\pi}\int \frac{d^2K}{(2\pi)^2}k_o^2\tilde{g}(K)\,V'(z_1)V'(z_2)\,e^{iKR_p}\times\int d\hbar\omega\frac{\mathrm{Im}R^{RPA}(K,\omega)}{E_o-\hbar\omega}. \tag{26}$$

In Fig. 4, the Fourier transform $\Delta(z_1,z_2,k_p)$ of the quantity $\Delta(z_1,z_2,R_p)$, in a direction parallel to the surface, and setting $k_p=0$, is shown as a function of the z_2 coordinate of one of the two particles, given to the other coordinate z_1 a fixed value. As expected, the probability that the two partners of a Cooper pair are close together, and thus that the associated pairing gap is large, is higher at the surface of the slab than elsewhere.

[1] C. Mahaux, P.F. Bortignon, R.A. Broglia, and C.H. Dasso, Phys. Rep. **120**, 1 (1985).
[2] P. Donati, T. Døssing, Y.R. Shimizu, S. Mizutori, P.F. Bortignon, and R.A. Broglia, Phys. Rev. Lett. **84**, 4317 (2000).
[3] G. Grimvall, *The Electron-Phonon Interaction in Metals* (North-Holland, Amsterdam, 1981).
[4] F. Barranco, R.A. Broglia, G. Gori, E. Vigezzi, P.F. Bortignon, and J. Terasaki, Phys. Rev. Lett. **83**, 2147 (1999).
[5] H. Esbensen and G.F. Bertsch, Ann. Phys. (N.Y.) **157**, 255 (1984).
[6] H. Esbensen and G.F. Bertsch, Phys. Rev. Lett. **52**, 2257 (1984); Phys. Lett. B **161**, 248 (1985).
[7] A. Bohr and B.R. Mottelson, *Nuclear Structure,* Vol. II (Benjamin, New York, 1975).
[8] A. Bohr and B.R. Mottelson, *Nuclear Structure*, Vol. I (Benjamin, New York, 1969).
[9] G. Audi and A.H. Wapstra, Nucl. Phys. A **595**, 409 (1995).
[10] N. Giovanardi, P. Donati, P.F. Bortignon, and R.A. Broglia, Ann. Phys. (N.Y.) **283**, 308 (2000).
[11] M. Tinkham, *Introduction to Superconductivity* (McGraw-Hill, New York, 1996).